MacAlpine Hills 88104, 88105

Anorthositic regolith breccia

61, 663 g

Figure 1: Interior photo of MAC 88105 showing a large feldspathic clast in the two halves.

Introduction

MacAlpine Hills (MAC) 88104 and 88105 (Fig. 1) were found by the 1988 ANSMET field team on January 13, 1989 in the eastern part of the MacAlpine Hills blue ice basin (Fig. 2). These meteorites were classified as anorthositic lunar meteorites by Score and Mason (1989) and Score et al. (1989). Each is covered with thin grey-green fusion crust. Other exterior surfaces are dark grey, and weathered. The interior is blue grey and fine grained or glassy in areas (Takeda et al., 1991).

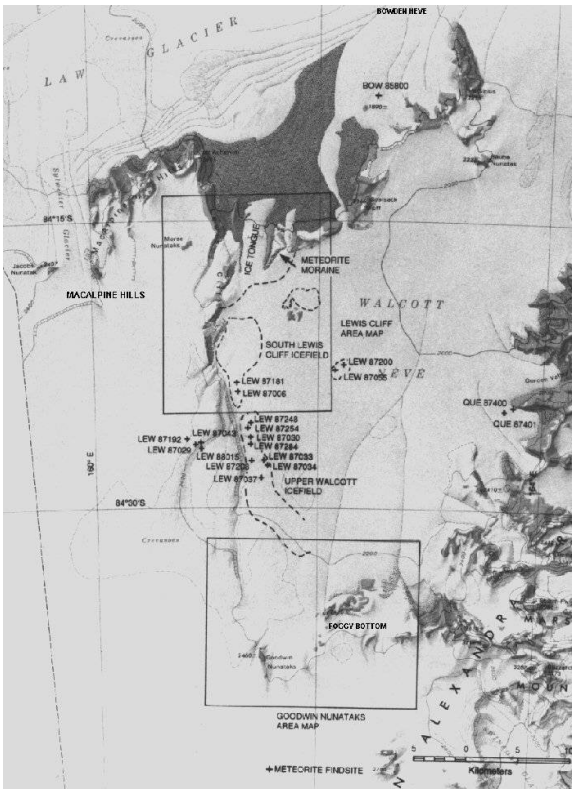

Figure 2: Location map for the Queen Alexandra Range and MacAlpine Hills regions of the Transantarctic Mountains.

Petrography

Both meteorites are polymict breccias that contain small clasts and lithic fragments in a brown glassy matrix. Most mineral grains are plagioclase feldspar, but there are also minor olivine, pyroxene, spinel. Although it has been noted that there is a lack of highland rock fragments, granulitic clasts, and Fe-rich mare basalt clasts compared to other lunar regolith breccias (Takeda et al., 1991), there is some heterogeneity and variability from sample to sample. For example, Neal et al. (1991) report on several granulitic highland clasts of FAN affinity as well as basaltic and impact glass beads (Figs. 3-5). Similarly, Delano (1991) compares the sparse, but present, impact glasses of MAC 88104/5 with those from Apollo 16 and ALH A81005. And, Jolliff et al. (1991) make a detailed report of a troctolite clast (among others) observed in MAC 88105.

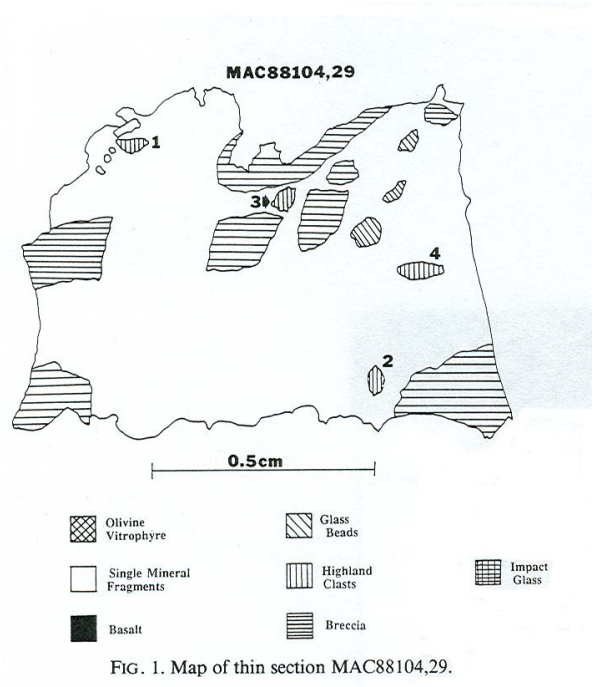

Figure 3: Sketch of section of MAC 88104,29, reported by Neal et al. (1991), and illustrating the diversity of lithologies in this meteorite.

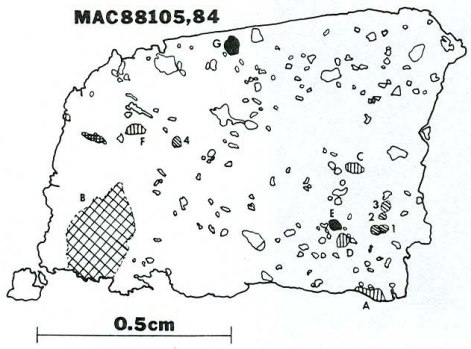

FIG. 3. Map of thin section MAC88105.84. Shading as in Fig. 2.

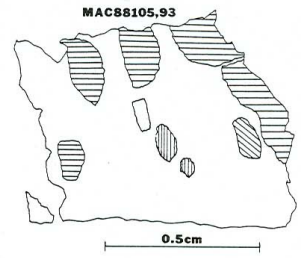

FIG. 5. Map of thin section MAC88105,93. See Fig. 2 for ke shading.

Figure 4 and 5: Sketch of section of MAC 88105,84 and MAC 88105,93 as reported by Neal et al. (1991), and illustrating the diversity of lithologies in two other sections of these meteorites.

Table 1: Modal mineralogy of MAC 88105

	Jolliff 91	Palme 91
split	80	8
Lithic clasts		
Vitric and recrystallized matrix melt breccias		30.7
Brown vitric matrix	43.2	-
Mafic, dark matrix	1.1	-
Intersertal/subophitic melt rocks/breccias		
Feldspathic melt rocks	1.4	6.5
Mafic melt rocks/basalts	0.3	15.7
Granultic breccias		21.0
granoblastic	1.6	-
poikiloblastic	2.0	-
Igneous fragments	2.5	-
Other	1.9	8.2
Mineral fragments		
Plagioclase	6.1	5.6
Mafic minerals	1.2	1.3
Glasses		11.0
Glass veins	0.8	-
Glass clasts	1.1	-
Matrix	36.8	-

Mineralogy

The pyroxenes in lithic clasts and fragments from MAC 88105 exhibit extensive solid solution between augite and low Ca pyroxene, with an Mg# range from 0.50 to 0.90 (Fig. 6). The plagioclase and mafic mineral compositions are at the high Mg# end of the trend for FAN's (Fig. 7), with very Ca-rich plagioclase. Despite the high Mg# compared to FAN's, it nonetheless has the lowest Mg# of highland meteorites. And the composition of olivine in troctolitic, noritic and anorthositic clasts is between Fo_{25} and Fo_{60} (Fig. 8).

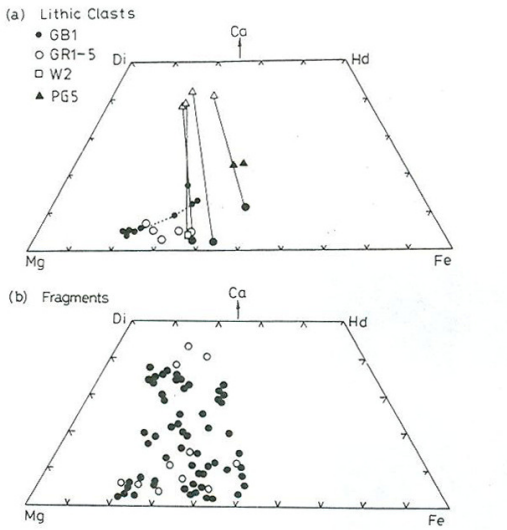

Figure 6: Pyroxene compositions for lithic clasts and fragments (from Takeda et al., 1991).

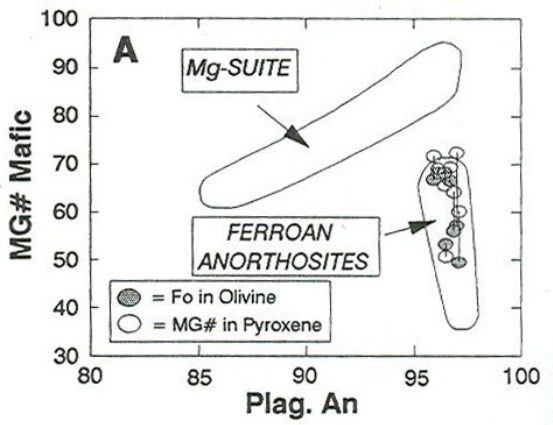

Figure 7: Plot of plagioclase composition (An) vs. mafic mineral Mg# for MAC 88105 compared to Apollo Mg-suite and FAN's (from Neal et al., 1991).

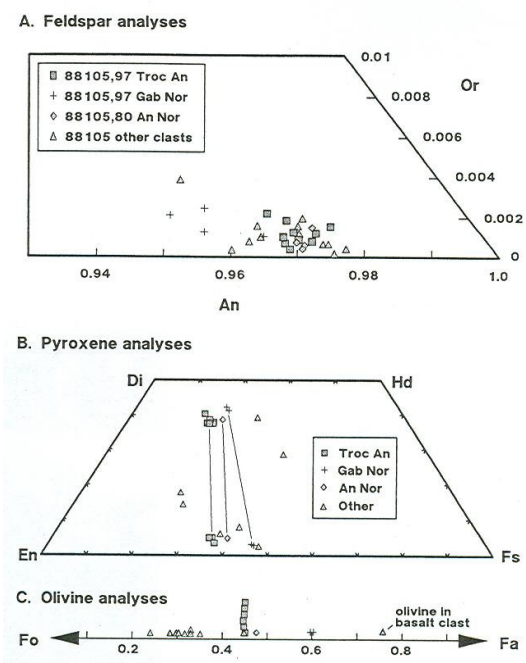

Figure 8: Plagioclase, pyroxene, and olivine compositions from clasts from MAC 88105 (from Jolliff et al., 1991).

Chemistry

The chemical composition of MAC 88105 is distinct in several ways. First, the Fe/Mn ratio of mafic minerals lies solidly in the lunar field, as defined by Laul et al. (1973). Second, the rare earth element pattern for the bulk rock show that MAC 88105 is low if REE, and similar to and overlaps with the high REE end of the FAN field (Fig. 9; Nyquist et al., 2002; Palme et al., 1991). Similarly, MAC 88105 falls at the low Al end of the lunar highland meteorites, and is also low in Sm, plotting off the trend of Sm-Al defined by a large range of lunar materials (Fig. 10; Warren and Kallemeyn, 1991). In terms of highly and moderately siderophile elements, MAC 88105 contains roughly 2x chondritic values of Re, Os, Ir, Ni, Au and Ge (Fig. 11). Finally, the noble gas content of MAC 88105 is also very low compared to other highlands meteorites (Fig. 12), and correlated with the low modal percentage of regolith indicators such as glass (Palme et al., 1991).

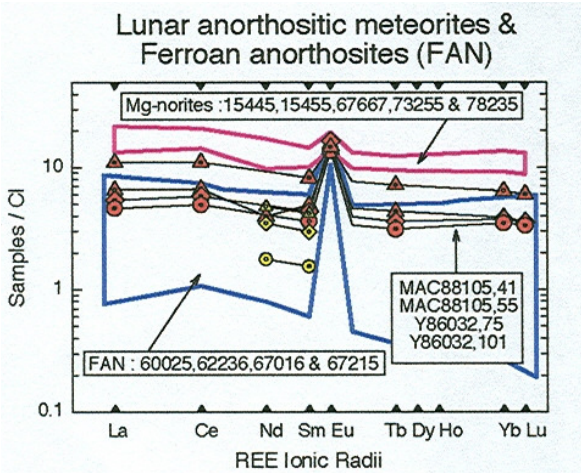

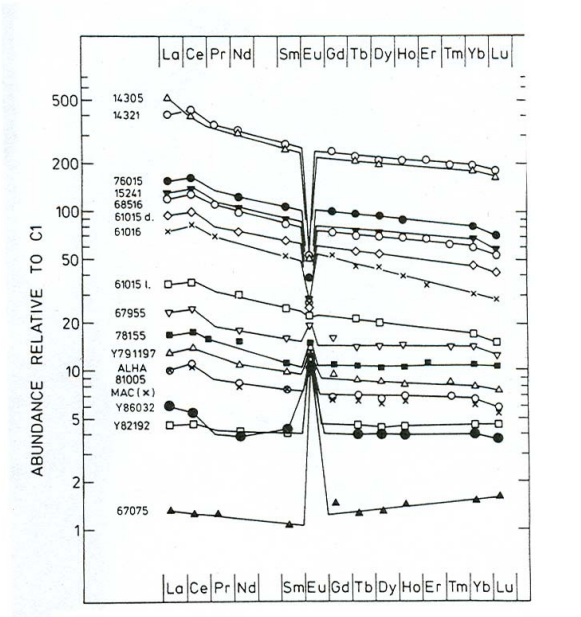

Figure 9A: Rare earth element analyses for clast W-1 in MAC 88105, from Nyquist et al. (2002); Figure 9B: Rare earth element analyses for bulk rock MAC 88105 showing a positive Eu anomaly as well as the overall low REE compared to Apollo samples, but similar to other highland meteorites (ALH A81005, Y86032, and Y82192), from Palme et al. (1991).

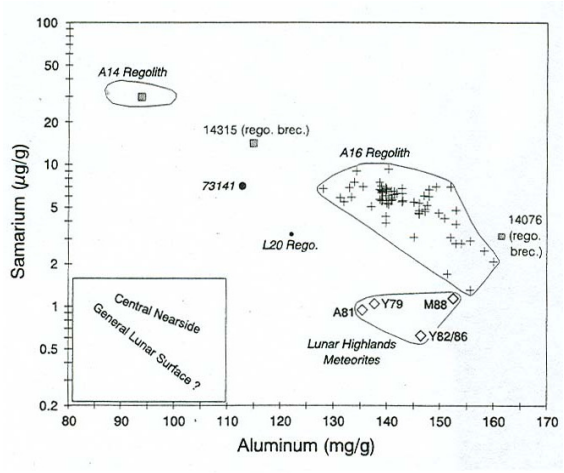

Figure 10: Sm-Al systematics for lunar samples, showing the low Sm and Al of MAC 88105, from Warren and Kallemeyn (1991).

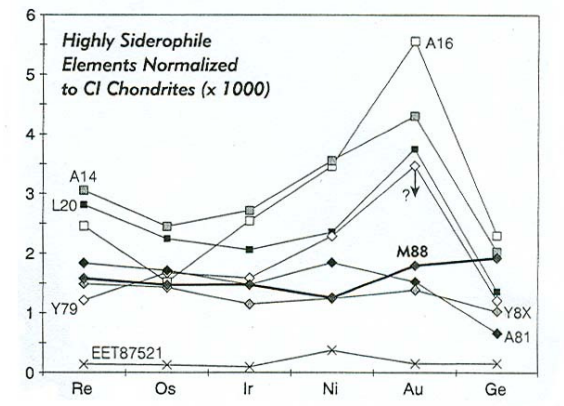

Figure 11: Bulk siderophile elements concentrations for MAC88105, from Warren and Kallemeyn (1991).

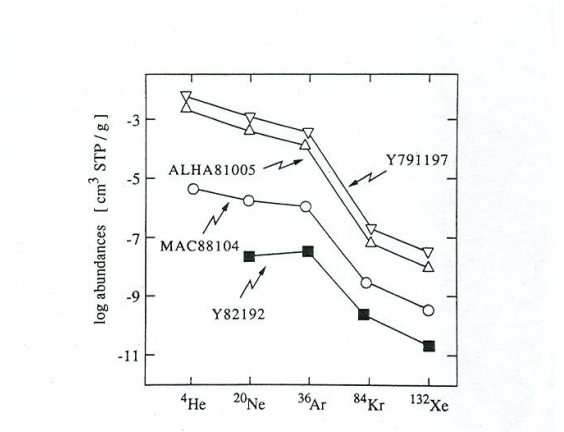

Figure 12: Noble gas concentrations in MAC 88104 compared to ALH A81005, Y791197, and Y82192, from Palme et al. (1991).

Table 2a. Chemical composition of MAC 88105

reference	1	1	1	2	3	3	4	4	5	6
Wt. mg	2.7	124.6	60.1	193.03	153.4	55.2	69.5	106.3	96.7	333
method	e	e	e	e	e	e	e	e	e, g	e
SiO_2 %							45.2	45.2		44.71
TiO_2	0.41	0.25	0.22				0.24	0.24	0.23	0.25
Al_2O_3	32.9	27.5	27.9				28.3	28.3	25.71	28.52
FeO	2.94	3.9	3.8	4.35	4.3	4.58	4.27	4.29	3.89	4.37
MnO	0.047	0.058	0.056		0.067	0.079	0.066	0.066	0.055	0.066
MgO	5.7	3.2	4.6				4.17	4.17	4.15	4.06
CaO	17.7	17.2	18.5	16.8			16.9	16.9	15.25	17.07
Na_2O	0.327	0.316	0.376	0.334	0.39	0.4	0.335	0.335	0.29	0.33
K_2O					0.023	0.022	0.034	0.034	0.025	0.026
P_2O_5	0.02	0.022	0.024						0.024	
S %										
sum										
Sc ppm	5.8	7.9	7.6	8.47	8.64	9.71	8.8	8.83	7.7	8.9
V	37	17	21						16	<34
Cr	700	490	550	638	655	738	623	622	620	640
Co	7.3	11.2	11.3	14.51	16.1	16.7	14.65	14.65	15.1	14.4
Ni		110	120	150	163	155	150	160	170	127
Cu										
Zn					12	10			18	7.6
Ga					4.12	3.6			3.22	3.51
Ge										780
As					0.06	0.08			0.15	
Se					0.26	0.22			<0.5	
Rb					0.9	<2			1.11	
Sr		130	120	156	150	200	170	150	149	150
Y									8.02	
Zr				34	44	40	30	38	30	35
Nb									1.8	
Mo									1.8	
Ru										
Rh										
Pd ppb										
Ag ppb										
Cd ppb										6.3
In ppb										
Sn ppb									440	
Sb ppb					40	<60				
Te ppb										
Cs ppm				0.04	0.059	0.062	0.05	0.04	0.031	
Ba		31	41	31	25	26	39	34	27	30
La	3.8	1.92	2.48	2.48	2.54	2.93	2.59	2.59	2.2	2.68
Ce	9	5.7	6.6	6.38	6.41	7.56	6.66	6.71	5.34	6

Pr									0.716	
Nd		3.2	3.4		4.1	5	4.3	5	3.11	3.7
Sm	0.271	0.88	1.12	1.203	1.22	1.46	1.203	1.23	1.08	1.13
Eu	1	0.8	0.82	0.79	0.77	0.8	0.824	0.834	0.73	0.81
Gd					1.3	1.65			1.01	
Tb		0.23	0.28	0.251	0.26	0.29	0.261	0.267	0.21	0.229
Dy		1.4	1.7		1.71	1.9			1.49	1.48
Ho									0.3	0.33
Er									0.84	
Tm									0.13	
Yb	0.34	0.75	1.03	0.987	1.05	1.18	1.05	1.03	0.87	0.98
Lu	0.069	0.113	0.145	0.138	0.16	0.18	0.147	0.146	0.125	0.143
Hf		0.65	0.87	0.9	0.88	0.97	0.93	0.95	0.75	0.78
Ta		0.1	0.12	0.112	0.087	0.096	0.117	0.113	0.085	0.103
W ppb					200	100			330	
Re ppb										0.59
Os ppb										0.0064
Ir ppb		9	10	7.7	5.8	6.9	6.6	6.3	6	11.2
Pt ppb										
Au ppb		3	4	2.7	3.5	4	2.3	2.1	4.6	1.78
Th ppm		0.3	0.44	0.42	0.33	0.41	0.44	0.42	0.33	0.36
U ppm				0.1	0.095	0.11	0.11	0.12	0.11	0.097

technique (a) ICP-AES, (b) ICP-MS, (c) IDMS, (d) Ar, (e) INAA, (f) RNAA, (g) SSMS

Table 2b. Light and/or volatile elements for MAC 88105

Li ppm			3.2
Be			
Be			
C			
S			
F ppm			48
Cl			382
Br	0.12	<0.12	0.132
I			1.6
Pb ppm			0.73
Hg ppb			
Tl			
Bi			

References: 1) Neal et al. (1991); 2) Jolliff et al. (1991); 3) Koeberl et al. (1991); 4) Lindstrom et al. (1991); 5) Palme et al. (1991); 6) Warren et al. (1991)

Radiogenic age dating

Argon dating of clast W-1 by Bogard et al. (2000) resulted in a plateau age of 4.07 ± 0.04 Ga (Fig. 13). Sm-Nd isotopic analysis of the same clast by Nyquist et al. (2002) results in model ages that are equally old, and negative εNd values which support an early lunar magma ocean (Nyquist et al., 2002).

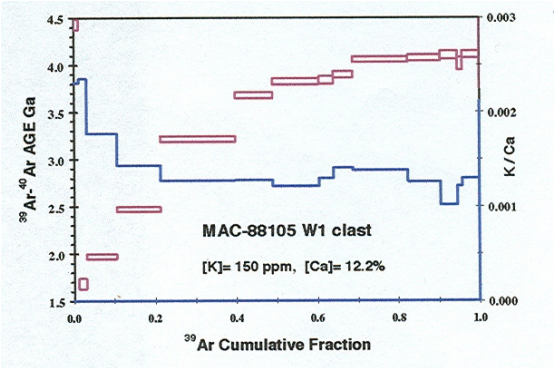

Figure 13: Ar plateau age for clast W-1 of MAC 88105, reported by Bogard et al. (2000).

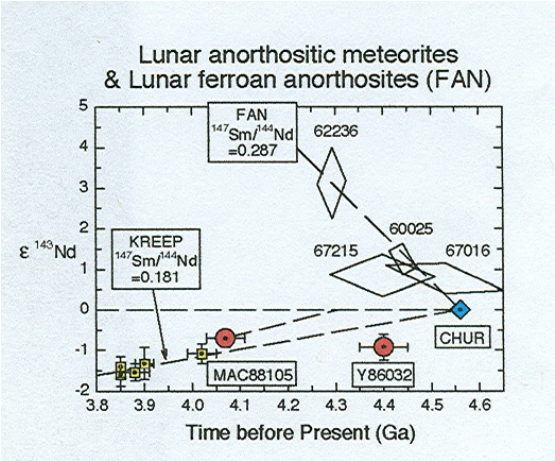

Figure 14: Sm-Nd isotopic constraints on the age of clast W-1 in MAC 88105, reported by Nyquist et al. (2002).

Cosmogenic isotopes and exposure ages

Measurements and modeling of the cosmogenic isotopes ^{10}Be, ^{26}Al, ^{36}Cl and ^{81}Kr result in lunar ejection ages of 0.21 to 0.64 for MAC 88105 (Eugster et al., 1991). These are in agreement with those determined by Nishiizumi et al. (1991), who also determined Earth-Moon transport times of 0.04 to 0.05 Ma, and terrestrial ages of 0.21 to 0.25 Ma (Nishiizumi et al., 1991).

Processing

At the time it was originally processed, MAC 88105 was the largest lunar meteorite, weighing in at 660 g (Figure 15). Initial processing of MAC 88105 produced chips ,4 and ,8 that were used for thermoluminescence and oxygen isotope analysis. (Table 3). In addition, the meteorite was divided roughly into two halves, with one half breaking into ,1 and ,2 (Figure 16). Split ,0 was subsequently slabbed into three pieces - ,9 ,10 and ,11 – (Figure 17). Split ,11 was divided into many chips for consortium and other detailed studies (Figures 18 and 19). The results of many of these studies were reported in a special issue of Geochimica et Cosmochimica Acta (vol. 55).

MAC 88104 has also been studied in some detail (Figure 20), although not nearly as many splits of 104 have been allocated (Table 4).

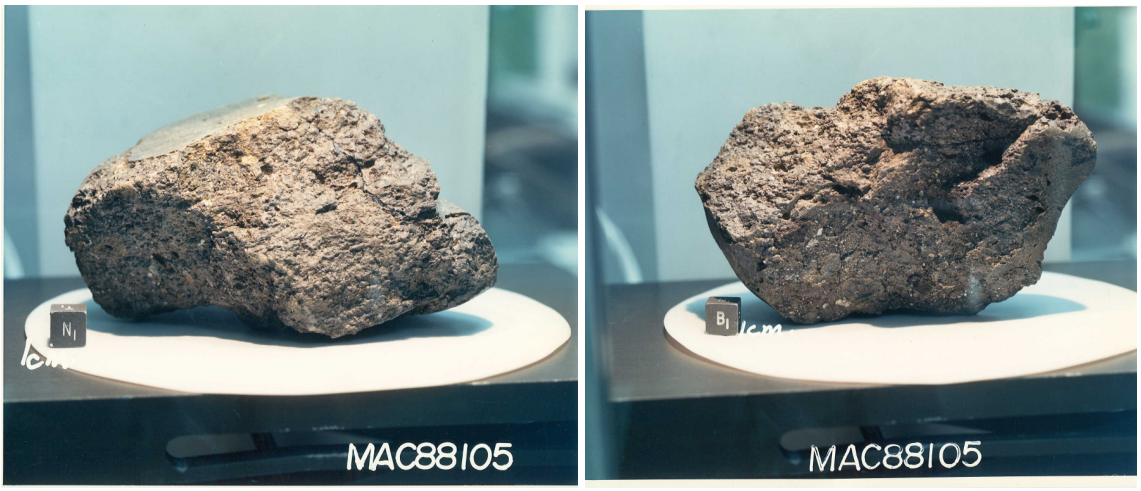

Figure 15: Four different views of MAC88105, taken in the Meteorite Processing Lab at NASA-JSC.

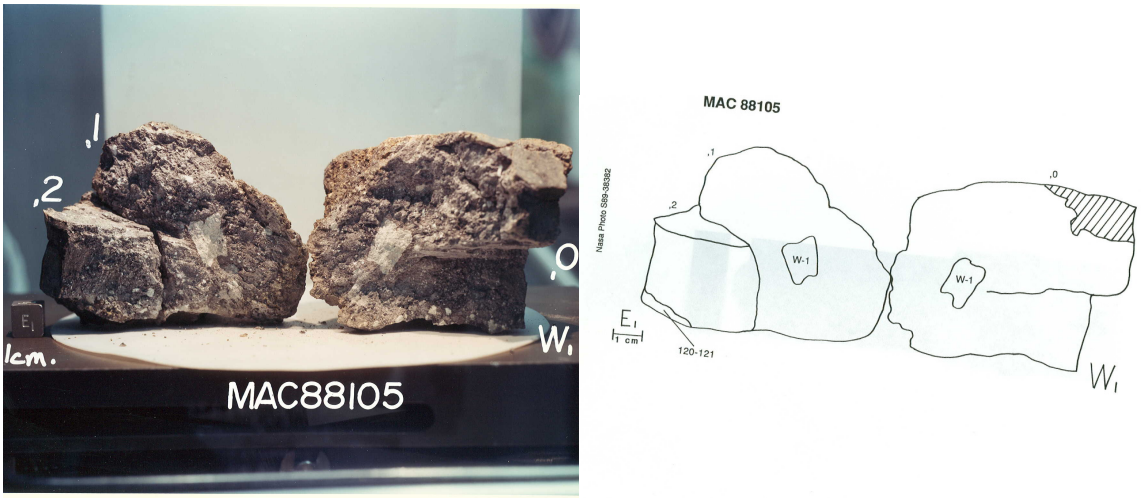

Figure 16: Photograph and sketch of two "halves" of MAC88105 generated during early processing.

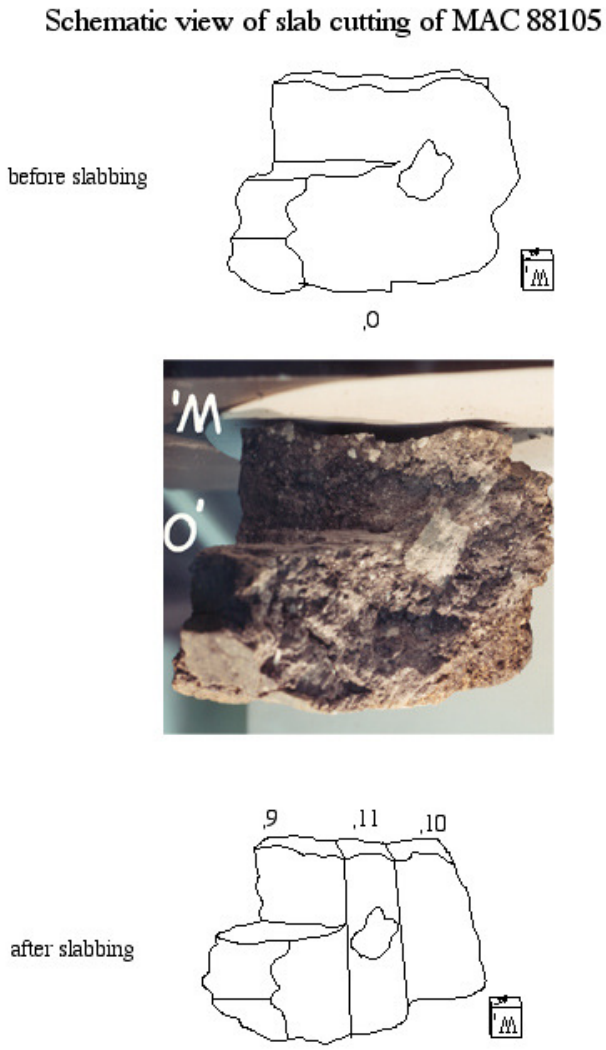

Figure 17: Sketches and photograph illustrating the slabbing of ,0 into ,9 ,10 and ,11.

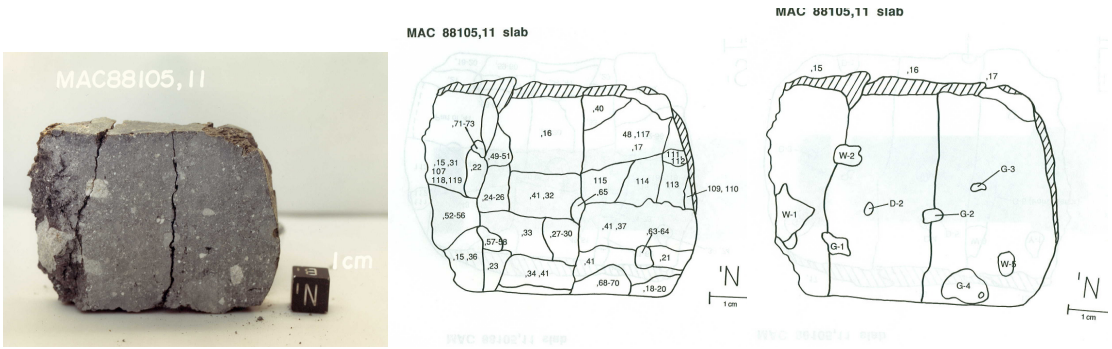

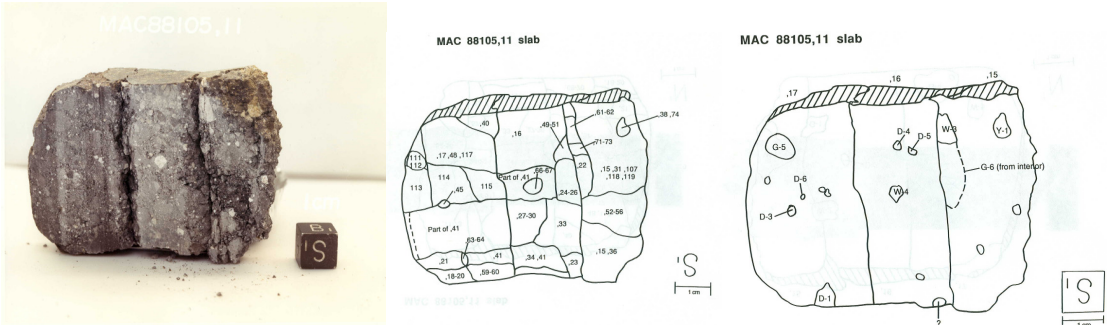

Figure 18: Two photographic views and accompanying sketches (by Carol Schwarz) illustrating the splits generated for allocation from the slab ,11. Most of the splits generated during this phase of processing were part of the consortium studies (Table 3 and Figure 19).

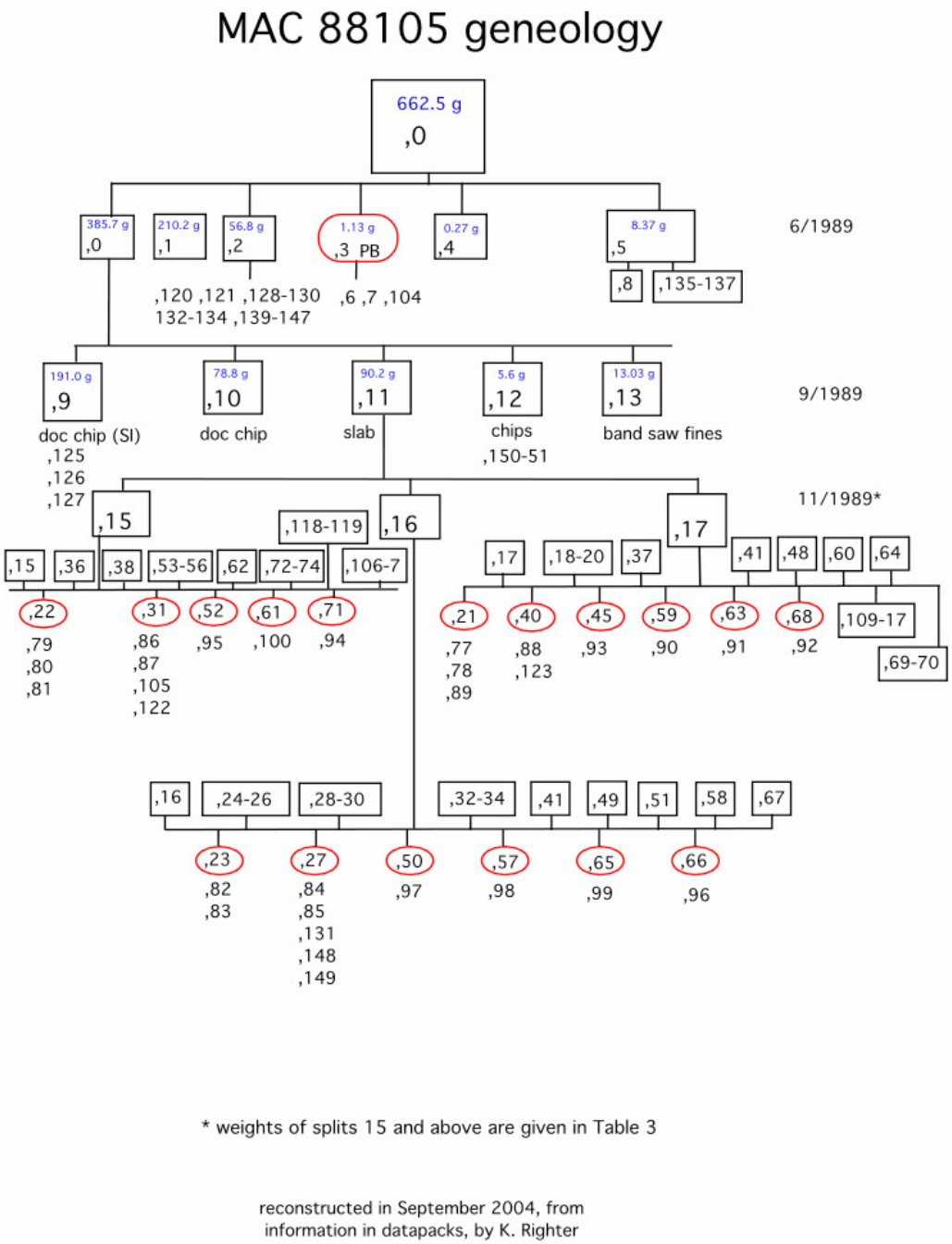

Figure 19: Genealogy of MAC 88105 showing chips as black rectangles and potted butts as red ovals.

Table 3: Splits of MAC 88105 generated during processing and allocation

split	parent	section	Wt. (g)	location	description
2	0		56.115	JSC	Documented chip
15	11		6.413	JSC	Slab chips w/clast Wl
16	11		10.49	JSC	Slab chip
17	11		16.797	JSC	Slab chip

18	11		0.285	JSC	Exterior chips
19	11		0.254	Nishiizumi	Exterior chip
20	11		0.06	Gooding	Exterior chip
21	11		1.175	TS chip	Matrix, with exterior
		77		JSC	
		78		Keil	
		89		Lindstrom	
22	11		1.511	TS chip	Matrix, interior
		79		Drake	
		80		Haskin	
		81		Delaney	
23	11		0.716	TS chip	Matrix, interior
		82		Delano	
		83		Takeda	
24	11		0.524	Eugster	Matrix, >1 cm from exterior
25	11		0.202	Nishiizumi	Interior chip
26	11		0.366	Eugster	Interior chip
27	11		1.122	TS chip	Matrix, interior
		84		Taylor	
		85		Palme	
		131			
		148			
		149			
28	11		1.044	Koeberl	Interior chips
29	11		0.229	Grady	Interior chips
30	11		0.096	JSC	Interior chips
31	11		1.667	TS chip	Matrix
		86		Warren	
		87		Koeberl	
		105		JSC	
		122		Barsukov	
32	11		0.326	Palme	Interior chips
33	11		5.04	Delano	Interior chip
34	11		0.379	Warren	Interior chip
35	11		1.044	Haskin	Chips w/clasts
36	11		0.063	Takeda	Chips w/glass
37	11		0.075	Takeda	Chips, avoided glass
38	11		0.018	Gooding	Clast Yl
39	11		0.105	Gooding	Matrix, interior, w/glass
40	11		0.787	TS chip	Chip w/dark f.c. (Gooding)
88				Gooding	
123				Haskin	
41	11		20.474	Jarosewich	In cps from different areas

42	11		0.521	Lindstrom	Matrix chips
43	11		0.108	Lindstrom	Matrix chip for TEM
44	11		0.27	JSC	Matrix interior
45	11		0.238	TS chip	D3 and matrix
		93		Taylor	
46	11		5.105	JSC	Chips and fines
47	11		3.679	JSC	Chips and fines
48	11		4.073	JSC	Chips and fines
49	11		0.005	Takeda	W2 chips
50	11		0.034	TS chip	W2 and matrix
		97		Haskin	
51	11		0.066	Haskin	W2 and matrix
52	11		0.098	TS chip	Wl and matrix
		95		Warren	
53	11		0.519	Nyquist	Wl clast chips
54	11		0.113	Warren	Wl clast chips
55	11		0.129	Lindstrom	Wl clast chips
56	11		2.055	JSC	Wl and matrix
57	11		0.021	TS chip	Gl clast chip
		98		Lindstrom	
58	11		0.084	Lindstrom	Gl and matrix
59	11		0.02	TS chip	Dl and matrix
		90		Lindstrom	
60	11		0.093	Lindstrom	Dl and matrix
61	11		0.015	TS chip	W3 and matrix
		100		Warren	
62	11		0.108	Warren	W3 and matrix
63	11		0.131	TS chip	W5 and matrix
		91		Warren	
64	11		0.101	Warren	W5 and matrix
65	11		0.01	TS chip	G2 and matrix
		99		Taylor	
66	11		0.024	TS chip	W4 and matrix
		96		Taylor	
67	11		0.02	Taylor	W4 and matrix
68	11		0.082	TS chip	G4 and matrix
		92		Taylor	
69	11		0.174	Taylor	G4 clast chips
70	11		0.64	JSC	G4 and matrix
71	11		0.034	TS chip	G6 and matrix
		94		Taylor	
72	11		0.098	Taylor	G6 and matrix
73	11		0.071	JSC	G6 and matrix

74	11		0.085	JSC	Yl and matrix
75	11		0.068	JSC	Chips and fines
106	15		0.133	Goswami	Wl and matrix
107	15		0.22	Goswami	Matrix chips
108	74		0.029	Haskin	Yl and matrix
109	17		0.151	Goswami	Exterior chip
110	17		0.102	Haskin	Exterior chip
111	17		0.101	Goswami	Dark melt clast?
112	17		0.157	JSC	Dark melt clast?
113	17		4.379	JSC	Slab chips
114	17		2.066	Barsukov	2 interior documented chips
115	17		2.435	JSC	Interior documented chip
116	17		1.204	JSC	Chips and fines
117	48		0.112	Haskin	Exterior chip
118	15		0.018	Goswami	Matrix chips
119	15		0.164	Goswami	Dark melt clast
120	2		0.122	Haskin	Exterior clast
121	2		0.563	JSC	Chips and fines
125	9		80.71	SI	Documented piece
128	2		0.028	Durrani	Interior chip
129	2		0.049	Durrani	Fusion crust
130	2		0.335	Gostin	3 chips with fusion crust
132	2		4.744	JSC	Chips and fines
133	132		0.025	Thomas	Interior chips
134	132		0.025	Thomas	Interior chips
135	5		0.030	Thomas	Exterior chips
136	5		0.030	Thomas	Exterior chips
139	2		0.147	Bada	Locatable interior chip
140	2		3.055	Humayun	Interior chips
141	2		2.040	Humayun	Exterior chips
144	2		0.120	Vogt	2 documented chips
145	2		0.120	Bada	Documented interior chip
150	12		0.017	Bizarro	chip

Table 4: Splits of MAC88104 generated during processing and allocation

split	parent	section	Wt. (g)	location	description
0	0		5.895	JSC	chips
1	0		1.750	JSC	Potted butt
		7		SI	Thin section
		8		Stöffler	Thin section
2	0		0.326	Sears	TL chip/IP
3	0		14.708	JSC	documented chip

4	0		9.903	JSC	documented chip
5	0		4.158	JSC	documented chip
6	0		11.902	JSC	chips
9	0		0.169	Nishiizumi	Locatable interior chip
10	0		0.263	Herzog	Locatable interior chips
11	0		0.502	Eugster	Interior chips
12	0		0.319	Palme	Interior chips
13	0		0.032	Grady	Interior chip
14	0		0.255	Lindstrom, M.	Interior chips
15	0		0.240	Haskin	Interior chips
16	0		0.468	JSC	Interior chips (returned)
17	0		1.433	JSC	Potted butt
		29		JSC	Thin section
		30		JSC	Thin section
18	0		1.885	JSC	Potted butt
		31		JSC	Thin section
		32		JSC	Thin section
19	0		1.803	JSC	Documented chip
20	0			JSC	Potted butt
		33		JSC	Thin section
21	0		0.228	JSC	B1 + matrix chips
22	0		0.331	JSC	W1 + matrix chips
23	0		0.017	JSC	Fusion crust
24	0		0.598	JSC	Interior chips
25	0		1.406	JSC	Chips with fusion crust
26	0		1.725	JSC	Chips and fines
27	0		0.023	JSC	Potted butt
		34		JSC	Thin section
36	24		0.223	Goswami	3 interior chips
41	16		0.073	Laul	Chip (consumed)
42	25		0.299	Sears	Exterior chips
43	24		0.072	Podosek	Interior chips

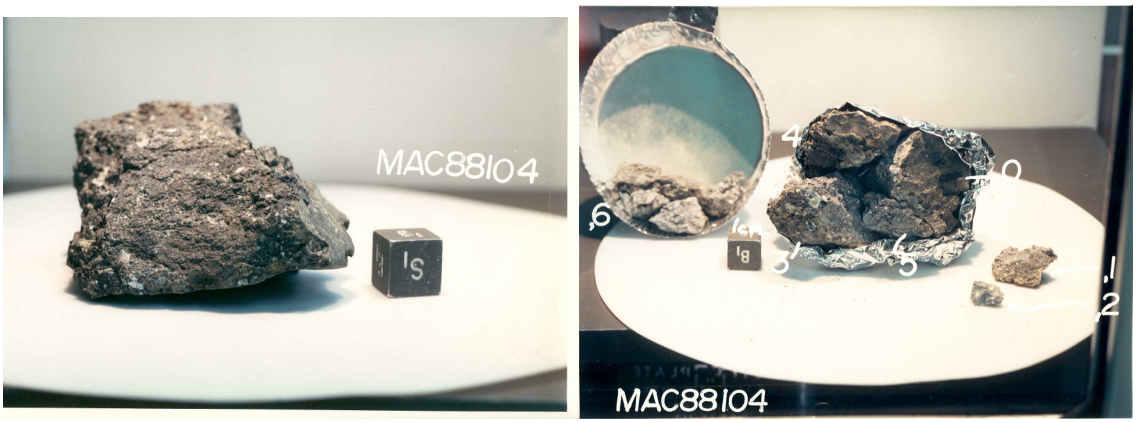

Figure 20: Early processing of MAC 88104.

K. Righter – Lunar Meteorite Compendium - 2010